



KINETIC, EQUILIBRIUM AND THERMODYNAMIC STUDIES ON ADSORPTION OF ACID RED 1 FROM AQUEOUS SOLUTION USING ACTIVATED TAMARIND KERNEL POWDER



A. D. Adams^{1*}, C. Enyeribe¹, B. Kadanga², H. Zubair² and M. O. Arogundade²

¹Department of Polymer & Textile Science, Ahmadu Bello University, Zaria, Nigeria

²Department of Science Technology, Nigerian Institute of Leather & Science Technology, Zaria, Nigeria

*Corresponding author: abrahamdanladiadams@gmail.com

Received: July 04, 2019 Accepted: November 16, 2019

Abstract: Activated tamarind kernel powder (ATKP) was prepared from tamarind fruit (*Tamarindus indica*) and utilized for the removal of Acid Red 1 (AR 1) from its aqueous solution. The powder was activated using 4N HNO₃. The adsorbent was characterised using infrared spectroscopy, bulk density, Ash content, pH, moisture content and dry matter content measurements. The effect of various parameters which include; temperature, pH, adsorbent dosage, ion concentration, and contact time were studied. Four different equilibrium Isotherm models were tested on the experimental data but the Temkin isotherm model (R² values ranging between 0.913-0.987) was best-fitted into the experimental data. The pseudo-second order was best fitted into the experimental data with R² value of 0.999. The values of the activation energy (E) obtained indicated that the adsorption of AR1, on ATKP is a physical process. The negative free energy (ΔG) indicated that the adsorption process is feasible and spontaneous, the negative enthalpy (ΔH) indicated that the reaction is exothermic in nature and the negative entropy (ΔS) indicated that there is decreased randomness at the solid/solution interphase during the adsorption process. Therefore, activated tamarind kernel powder has proven to be a very good adsorbent (with removal efficiency ranging from 54 – 95%) for the removal of Acid Red 1 from industrial waste water.

Keywords: Acid red 1, isotherms, kinetics, tamarind, thermodynamics, waste water

Introduction

Environmental pollution control is said to be a matter of utmost concern in many countries. However, air and water pollution constitute the major environmental pollution in several countries. Consequently, open burning leads to air pollution, while industrial effluent and domestic sewage leads to water pollution. Water pollution results to bad effects on public water supplies which can cause health problem, while air pollution can cause lung diseases, burning eyes, cough, and chest tightness. The environmental issues surrounding the presence of colour in effluent is a continuous problem for dye stuff manufacturers, dyers, finishers, and water companies (Kesari *et al.*, 2011).

Textile and dyeing industry are among important sources for the continuous pollution of the aquatic environment. Because they produce approximately 5% of them end up in effluents. The textile and dyeing industries effluents are discarded into rivers, ponds and lakes; they affect the biological life various organisms (Ho and Mckay, 2003). Dye-containing effluents are undesirable wastewaters because they contain high levels of chemicals, suspended solids, and toxic compounds. Colour causing compounds can react with metal ions to form substances which are very toxic to aquatic flora and fauna and cause many water borne diseases (Vijayakumar *et al.*, 2012). Due to the chemical structure of dye, they are act as a resistant to many chemicals, oxidizing agents, and heat, and are biologically non-degradable. So it is difficult to decolorize the effluents, once released into the aquatic environment. Many of the methods are available for the removal of pollutants from water, the most important of which are reverse osmosis, ion exchange, precipitation and adsorption. Of these methods, adsorption technique is a most versatile and widely used technique (Mattson and Mark, 1971), because of its inexpensive nature and ease of use. Activated carbons are widely used because of their high adsorption abilities for a large number of organic compounds. However, the price of activated carbons is relatively high, which limits their usage (Bhattacharya and Sharma, 2005). This has led many researchers to search for cheaper substitutes such as coal, fly ash, silica gel, wool wastes, agricultural wastes, wood wastes,

and clay materials. They have been applied with varying success in dye removal (Akbal, 2005).

The present study was performed to investigate the surface morphology of activated tamarind kernel powder (ATKP) using various methods *viz*; FT-IR spectroscopy and exploitation for removal of Acid Red 1 from aqueous solution. The parameters such as pH, initial concentration, contact duration and adsorbent dosage with different temperature were studied. Adsorption isotherm models (Freundlich, Temkin, DubininRadushkevich and Langmuir) and adsorption kinetic models (Pseudo first-second-order) were also utilised.

Materials and Methods

Sample collection, identification and treatment

Tamarind kernel fruit was collected from the local market at Samaru, Sabongari Local Government Area of Kaduna state. The samples were taken to Biological Sciences Department of Ahmadu Bello University where it was identified as *Tamarindus indica* using the method described by Prescott (1977). The Tamarind kernel seeds were washed thoroughly with water to remove the adhering materials. Then, the reddish testa of the seeds was removed by heating seeds in an oven at 80°C for 2 h. The kernels were tamped and placed in the oven at a temperature of 300°C for 3 h for the tamped powder to carbonize completely. The powder was sieved through 400 microns to get uniform particle size for use. The Acid Red 1 dye sample was supplied by Sigma Aldrich Germany. Stock solution (1.0 g/L) of Acid Red 1 was prepared by dissolving about 1 gram of the dye in 1 litre of distilled water. All test solutions of the desired concentrations were prepared by successive dilutions to get the required initial Dye concentrations (20–100 mg/L).

Characterization of the adsorbent

The surface morphology of activated tamarind kernel powder was determined using infrared spectrophotometry. The pH of the adsorbent was obtained using standard test method ASTM D3838-80 (Andre *et al.*, 2011) and the ash content was determined using standard test method ASTM E1755-01 (ASTM, 1996; in Okoli *et al.*, 2015). The moisture and dry matter content of the adsorbent was determined using the method described in Gimba *et al.* (2009).

Batch adsorption experiment

The adsorption experiment was carried out by batch method. The experiment was carried out using 50 mL of adsorbate at ambient temperature (27°C) with a basic reciprocating shaker using 120 ml glass bottle as the reactor. The effect of initial dye concentration was analysed using an initial working dye concentrations are 20, 40, 60, 80 and 100 mg/L. The experiment was carried out using 0.2 g of the adsorbent, pH6 and at a contact time of 120 min. The effect of the adsorbent dosage was determined at a constant pH of 6, initial dye concentration of 20 mg/L and agitation time of 2 h. The adsorbent dosage was varied as follows: 0.4, 0.6, 0.8, 1.0 and 1.2., as described in Oladunni *et al.* (2012).

The effect of initial pH was determined by altering the pH at constant temperature (27°C), adsorbent dosage (0.2 g), initial concentration (20 mg/L) and agitation time (2 h). The pH was varied at 2, 4, 6, 8 and 10 using 0.1M HCl and 0.1M NaOH to either increase or decrease the pH of the solution (Oladunni *et al.*, 2012).

The effect of contact time is an important factor in adsorption studies as it helps in the study of the kinetics of adsorption. The effect of contact time was determined by agitating the mixture at varied time intervals. The agitation was carried out at constant temperature (27 °C), adsorbent dosage (0.2 g), initial concentration (20 mg/L) and pH (pH 6). The contact time was varied at 20, 40, 60, 80 and 100 min.

The effect of Temperature is important to this study as it helps in generating the data needed for adsorption thermodynamic study. This was determined by agitating the mixture at varying temperatures and initial dye concentrations. The agitation was carried out at constant adsorbent dosage (0.2 g), and pH (pH 6) and contact time. The different temperatures used were 298 K, 308, 318, 323 and 328 K (Oladunni *et al.*, 2012).

The concentration of the dye remaining in the solution was determined using an Agilent Cary 300 UV/visible spectrophotometer. The amount of dye adsorbed was calculated using the equation:

$$qe = V \frac{(Co - Ce)}{W} \quad (1)$$

Where: q_e is the amount of dye adsorbed by unit mass of the adsorbent, V is the volume of the solution, C_o is the initial dye concentration, C_e is the residual dye concentration and W is the weight of the adsorbent. The percentage dye removed (% Rem) was determined using the equation (Oladunni *et al.*, 2012).

$$\%Rem = \frac{(Co - ce)}{Co} \times 100 \quad (2)$$

Results and Discussion

The Physicochemical parameters obtained are presented in Table 1. The moisture content of a sample can be seen as the amount of water present in that sample. It has been reported that moisture content dilutes the activated carbon as such increases its weight during treatment process (Oladunni *et al.*, 2012). For this reason, it can be said that the lower the moisture content of an activated carbon the better its adsorptive capacity (Gimba *et al.*, 2009). Activated TKP is seen to possess 3.45% of moisture and 96.55% of Dry matter. The percentage of moisture was lower when compared to values obtained from *Khayasenegalensis* fruit (6.17 %) (Gimba *et al.*, 2009), walnut shell (4.18%) (Abechi, 2006), *Delonixregia* (6.286%) (Ocholi, 2006) and Locust bean husk (8.20%) (Oladunni *et al.*, 2012). The low moisture and high dry matter content of the ATKP indicates that the adsorbent is an excellent material for adsorption processes (Okoli *et al.*, 2015). The bulk density of activated Tamarind kernel powder was found to be 0.4 g/cm³ which showed some variation with that reported for locust bean husk (0.49 g/cm³) (Oladunni *et al.*, 2012), 0.26 g/cm³ for saw dust of *Dalbergiasisso*

(Shakirullah *et al.*, 2006); 0.81 g/cm³ for *Khayasenegalensis* fruits (Gimba *et al.*, 2009); 1.1034 g/cm³ for walnut shell (Abechi, 2006); 0.73 g/cm³ for rice husk carbon (Malik, 2003); 0.48 g/cm³ for *Euphorbia antiquorum* Palanisamy *et al.*, 2013); 0.28 g/cm³ for *Enteromorpha prolifera* (Sun and Yang, 2003); and 0.5494 g/cm³ for mosambi peel (Ladhe *et al.*, 2011). The amount of ash depends on the carbon sources or biomass (OMRI, 2002). The percentage ash content of the activated tamarind kernel powder was found to be 5.30%. Thus, the low ash content value indicates that the ATKP has low inorganic content and high fixed carbon. 2.08% was reported for Cornelian cherry, 2.21% for Apricot stone and 2.14% for Almond shells (Erhanet *et al.*, 2004); 23.0% was reported for Mosambi peel (Ladhe *et al.*, 2011); 3.72% for *Enteromorpha prolifera* (Deshuaiet *et al.*, 2013); 6.5% for saw dust carbon and 45.97 % for Rice husk carbon (Malik, 2003); 13.4% for *Euphorbia antiquorum L* (Palanisamy *et al.*, 2013); 2.58% for Wheat shells (Bulut and Aydin, 2006) and 3.50% for locust bean husk (Oladunni *et al.*, 2012). The pH of the activated Tamarind kernel powder was 6.45, and this happens to fall within the acceptable pH range for an ideal adsorbent. pH 6.30 was reported for rice husk carbon (Dada *et al.*, 2012); pH 7.7 for Mosambi peel (Ladhe *et al.*, 2011). pH 6.20, 6.25 and 5.80 for Cornelian cherry, Apricot stone and Almond shell, respectively (Erhan *et al.*, 2004).

Table 1: Physicochemical parameters of tamarind kernel powder

Parameters	ATKP
Dry matter content (%)	96.55
Moisture content (%)	3.45
pH	6.40
Bulk Density (g.cm ⁻¹)	0.40
Ash content (%)	5.30

FTIR analysis of ATKP

Fourier Transform Infrared Spectroscopy (FTIR) study was carried out to study and identify the functional groups present in the adsorbents ranging from 4000 to 650 cm⁻¹. The adsorption capacity or potential of an adsorbent depends upon its porosity as well as the chemical reactivity of the functional groups at the adsorbent surface (Suresh *et al.*, 1994). The spectra showing the functional groups and their peaks on the activated tamarind kernel powder and dyetreated activated tamarind kernel powder are presented. Furthermore, the results show the presence of Phosphates (P-O-C), (-C=C-Stretch alkenyl), (-C=C-Stretch conjugated), alkanes (C-H stretch), alkenes (=C-H stretch), alkynes (-C≡C-), carboxylic acids (O-H bend), aromatic amines (C-N), nitrites (C≡N stretch), aromatics (C-H stretch), alkyl halides, (C-O Stretch, Primary alcohol) etc. An observed shift in the wave number of dominant peaks associated with the spectra indicates the various functional groups activities on the activated tamarind kernel powder surface (Okoli *et al.*, 2015). These activities have been characterized by the interaction between the functional groups on the surface of the adsorbent and the functional groups in the dye molecule. A shift from 3261.4 cm⁻¹ on the ATKP spectrum (O-H stretch, carboxylic acid) to 3257.7 cm⁻¹ on AR 1 spectrum signifying an O-H (broad) stretch H-bonded, Hydroxyl group. A shift from 2922.2 cm⁻¹ on the ATKP spectrum signifying H-C-H stretch alkanes to 2926.4 cm⁻¹ on the AR 1 spectrum indicating methyl C-H asymmetric/symmetric stretch. A shift from 1699.7 cm⁻¹ on ATKP spectrum indicating the presence of -C=C-stretch alkenyl to 1703.4 cm⁻¹ on AR 1 spectrum indicating the presence of aromatic combination bands. A shift from 1237.5 cm⁻¹ on ATKP spectrum indicating the presence of C-N stretch aromatic amines to 1241.2 cm⁻¹ on AR 1 spectrum

indicating the presence aromatic ethers, Aryl-O stretch or aromatic phosphates (P-O-C stretch) (Table 2). The presence of hydroxyl groups, carbonyl groups, ethers, and aromatic compounds is an evidence of the lingo-cellulosic structure of

tamarind kernel powder which was also observed in other materials such as coconut shell (Andre *et al.*, 2011) and cotton stalks (El-Hendaway *et al.*, 2008; in Okoli *et al.*, 2015).

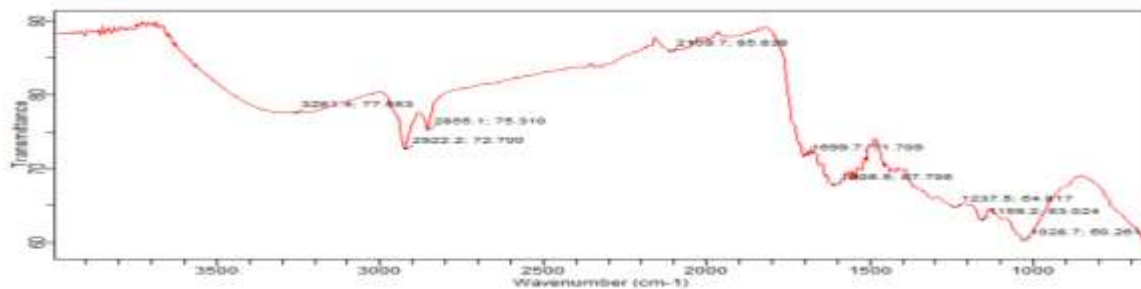


Fig. 1: FTIR spectrum of activated tamarind kernel powder

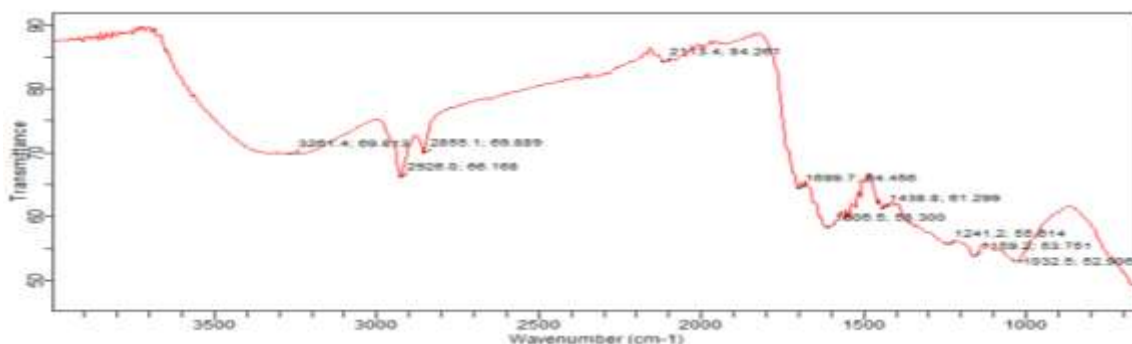


Fig. 2: FTIR spectrum of acid red 1 treated TKP

Table 2: FTIR analysis of AR1 adsorbed on ATKP

Group frequency (cm ⁻¹)	Functional group assignment
3261.4	O-H (broad) Hydroxyl group, H-bonded OH Stretch
2926.0	Methyl C-H asymmetric/symmetric Stretch
2855.1	Methyl C-H asymmetric/symmetric Stretch
2113.4	$\text{—C}\equiv\text{C—}$ terminal alkyne (monosubstituted)
1699.7	Aromatic combination bands
1606.5	Open chain Azo , Primary amine (NH bend)
1438.8	Aromatic nitro compounds
1241.2	Aromatic Phosphates (P-O-P stretch)
1159.2	$\text{—C}=\text{N}$ Stretch, tertiary amine
1032.5	C-O Stretch, Primary alcohol

Batch adsorption studies

Effect of pH

The effect of pH on the adsorption of AR 1 dye unto activated tamarind kernel powder was studied between the ranges of 2-10. The percentage of dye adsorbed decreased from 95.00 to 61.00% for Acid Red 1 as compared to Reactive Blue 29 and Reactive orange 20 dyes (Fig. 3).

It was observed that the percentage removal of dye increases rapidly with an increase in contact time initially, and thereafter, beyond a contact time of about 80 min, no noticeable change in the percentage removal was observed. When the contact time was increased from 20 to 100 min the percentage dye removal increased from 62.5 to 79.0%.

The initial concentration of adsorbate plays an important role, as a given mass of adsorbent can adsorb only a certain amount of a solute. The percentage removal of the dye depreciated with increase in initial dye concentration i.e. from 54.0 to 78.3%. The result indicated that the more the concentration of the solution, the smaller the percentage of dye that a given mass of adsorbent can adsorb (Okoli *et al.*, 2015). This is due to the fact that at lower concentrations, the amount of

available adsorption sites are more, while at higher concentrations, the available sites become less. The adsorption sites take the available dye molecules more rapidly at lower concentrations while at higher concentrations the molecules are required to diffuse to the adsorbent surface by intra particle diffusion (Oladunni *et al.*, 2012). Thus, the percentage of dye removal was dependent upon the initial concentration.

The results obtained from this experiment as presented indicated that as the adsorbent dosage increased (from 0.4 to 1.2 g) the percentage of dye adsorbed increased also from 65.0 to 86.0%. The percentage of adsorption increased up to 1.0g of adsorbent after which no significant changes in the percentages of dye adsorbed was observed with an increasing amount of the adsorbent. It has been reported that for every given initial concentration of an adsorbate, the adsorbent dosage determines the capacity of an adsorbent (Joseph and Philomena, 2011). It has also been reported that the increase in adsorption efficiency is as a result of the increased number of adsorption sites and surface (Okoli *et al.*, 2015). However, from the experiment, it was observed that equilibrium was attained after 1.0 g of adsorbent was used for the analysis.

Most of the adsorbents studied attained equilibrium around 1.0 g of dosage (Okoli *et al.*, 2015), but further increase in the adsorbent dose resulted in the reduction in the amount of dye removed from the solution. This resulted from the overlapping of the adsorption sites as a result of overcrowding of the

highest adsorbent dosage which has imposed a screening effect on the dense outer layer of the cells, thereby shielding the binding site from the dyes (Oladunni *et al.*, 2012).

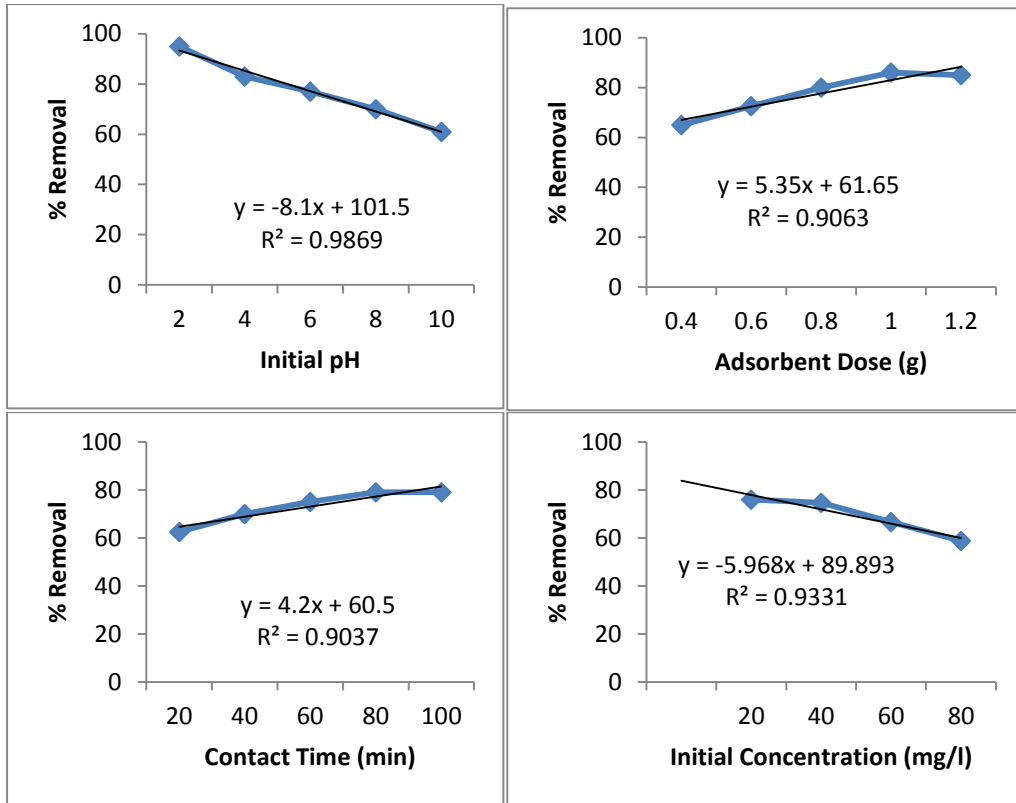


Fig. 3 Effect of initial pH, adsorbent dose, contact time, and initial concentration on % dye removal

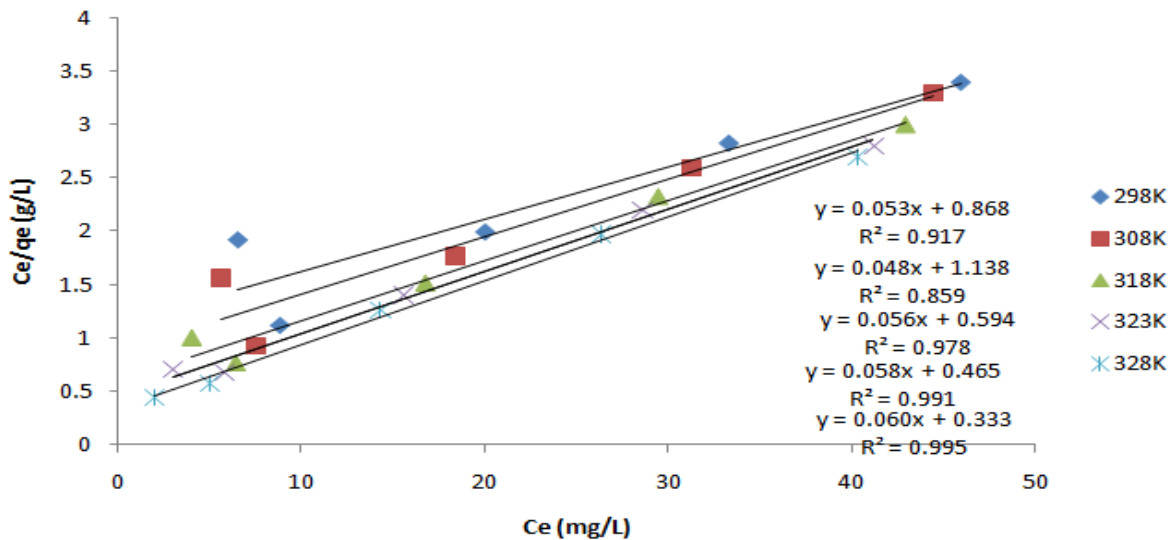


Fig. 4: Langmuir isotherm model for AR1 adsorption on ATKP

Langmuir isotherm model

The non-linear expression of Langmuir isotherm model can be illustrated as Equation (1) (Langmuir, 1916):

$$q_e = q_m K_L C_e / (1 + K_L C_e) \quad (3)$$

Where: C_e is the concentration of solution at equilibrium (mg/L); q_e is the corresponding adsorption capacity (mg/g); q_m (mg/g) and K_L (L/mg) are constants which are related to adsorption capacity and energy or net enthalpy of adsorption, respectively. Linear forms of the isotherms models are also

widely adopted to determine the isotherm parameters or the most fitted model for the adsorption system due to the mathematical simplicity. The linear form of the Langmuir is as follows:

$$C_e/q_e = 1/q_m K_L + C_e/q_m \quad (4)$$

Langmuir constants b and q_m represent the adsorption equilibrium constant and the maximum adsorption capacity, respectively. A straight line graph with slope of $1/q_m$ and

intercept b was obtained when C_e/q_e was plotted against C_e . From the Figures it could be seen that the plots are linear and the correlation coefficient (R^2) values were found to be 0.859, 0.917, 0.978, 0.991, and 0.995 at 298, 308, 318, 323 and 328 K, respectively which indicate that the graphs follow the Langmuir isotherm model (Fig. 4). The maximum adsorbate capacity (q_m) for Acid Red 1 were 20.8, 18.87, 17.86, 17.24, and 16.67 mg/g at 298, 308, 318, 323 and 328 K, respectively. From the results it could be seen that q_m , which also signifies the number of sites available for adsorption, is decreasing as the temperature increased from 298 to 328 K. The constant b relating to the coefficient of affinity of Acid Red 1 to activated tamarind kernel powder at 298, 308, 318, 323 and 328 K is 0.04, 0.06, 0.09, 0.13, 0.18 l/mg, respectively.

Separation factor R_L

The equilibrium parameter R_L , which is a dimensionless constant, is referred to as separation factor and is given by:

$$R_L = \frac{1}{1+(1+bC_0)} \quad (5)$$

Where: C_0 is the initial concentration and b is the Langmuir equilibrium constant. The R_L values indicate the adsorption to be favourable if ($0 < R_L < 1$), unfavourable if ($R_L > 1$), linear if ($R_L = 1$) or irreversible if ($R_L = 0$). The R_L values issued from this study were ranged from 0.05 to 0.35 for AR1 dyewith the increase in temperature from 298 to 328 K.

The result obtained from separation factor (R_L) calculation showed that adsorption of Acid Red 1 dye is favourable on activated tamarind kernel powder (Fig. 5).

Freundlich isotherm

The Freundlich adsorption isotherm [28] is given by:

$$q_e = K_f C_e^{1/n} \quad (6)$$

A linear form of the expression above is written as:

$$\log q_e = \log K_f + 1/n \log C_e \quad (7)$$

Where: q_e is the amount of adsorbate per unit weight of adsorbent, K_f is Freundlich constant measuring adsorption capacity, C_e is the equilibrium concentration of the adsorbate in solution, n is a constant related to adsorption efficiency and energy of adsorption intensity of adsorbent. K_f and n can be obtained from the intercepts and slopes of the linear plot of $\log q_e$ against $\log C_e$. From the figures it could be seen that the plots are linear and the correlation coefficient (R^2) values were found to be 0.803, 0.793, 0.863, 0.797, and 0.931 at 298, 308, 318, 323 and 328 K, respectively which indicate that the graphs follow the Freundlich isotherm model (Fig. 6). The adsorption capacity (K_f) of the activated tamarind kernel powder for Acid Red 1 were 1.57, 1.98, 2.93, 3.32, and 3.97 (l/g) at 298, 308, 318, 323 and 328 K, respectively. From the results it could be seen that K_f , which also signifies the adsorption capacity of the adsorbent, is increasing as the temperature increased from 298 to 328 K. The constant n relating to the adsorption efficiency of activated tamarind kernel powder for Acid Red 1 at 298, 308, 318, 323 and 328 K is 1.73, 1.88, 2.12, 2.27, and 2.66, respectively.

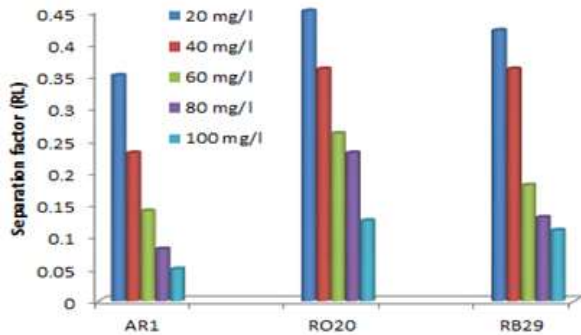


Fig. 5: Separation factor for AR1 adsorption on ATKP

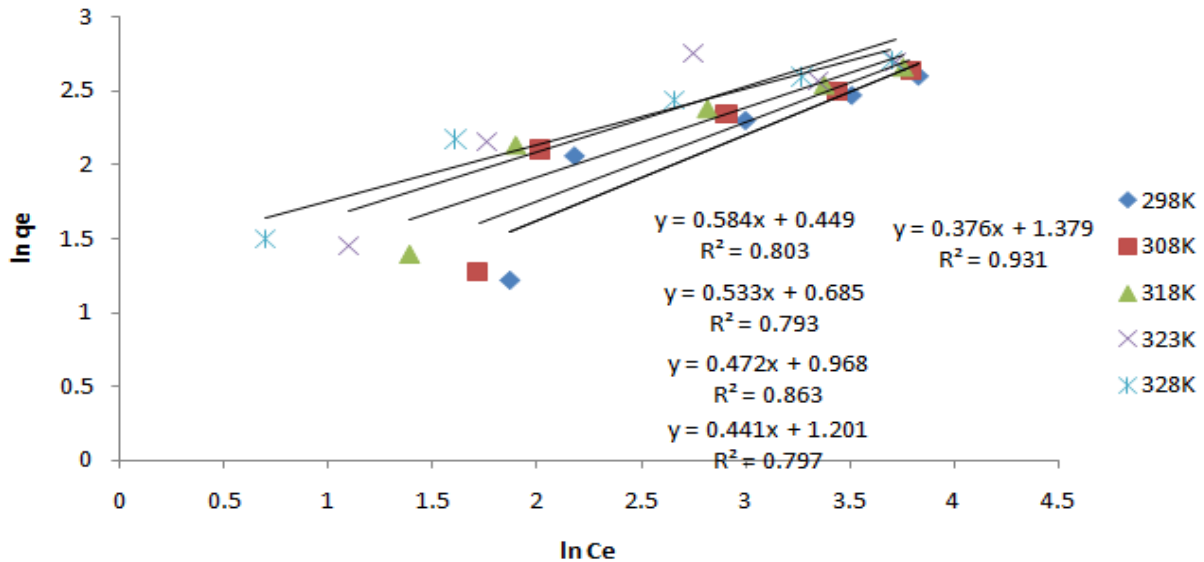


Fig. 6: Freundlich isotherm model for AR1 adsorption on ATKP

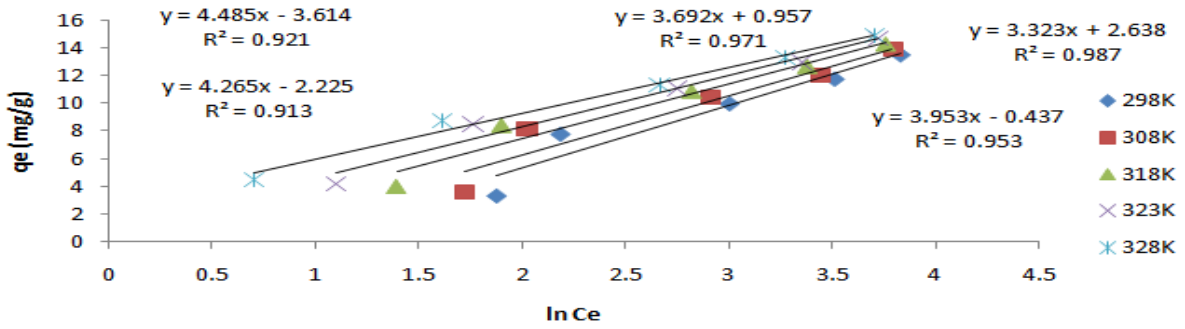


Fig. 7: Temkin isotherm model for AR1 adsorption on ATKP

Temkin isotherm

The linear form of Temkin isotherm can be expressed as:

$$q_e = (RT/b_T) \ln A_T + (RT/b_T) \ln C_e \quad (8)$$

Where: A_T is the Temkin isotherm equilibrium binding constant (L/g); b_T is the Temkin isotherm constant; R is the universal gas constant (8.314 J/mol/K), T is the temperature at 298 K; and C_e is the equilibrium concentration (mg/L). Temkin isotherm constant b_T and Temkin isotherm equilibrium binding constant A_T are obtained from the intercepts and slopes of the linear plot of q_e versus $\ln C_e$.

The Temkin isotherm equation assumes that the heat of adsorption of all the molecules in a unit layer decreases linearly with coverage due to adsorbent-adsorbate interactions, and that the adsorption is characterized by a uniform distribution of the bonding energies, up to some maximum binding energy.

Temkin isotherm constant b_T and Temkin isotherm equilibrium binding constant A_T were obtained from the intercepts and slopes of the linear plot of q_e versus $\ln C_e$. The Temkin adsorption isotherm models for Acid Red 1 at a temperature range of 298K to 328K respectively. From the figures it could be seen that the plots are linear and the correlation coefficient (R^2) values were found to be 0.803, 0.793, 0.863, 0.797, and 0.931 at 298, 308, 318, 323 and 328 K, respectively which indicate that the graphs follow the Temkin isotherm model. The adsorption capacity (A_T) of the activated tamarind kernel powder for Acid Red 1 were 2.27, 1.69, 1.12 l/g, 1.33, and 2.21 l/g at 298, 308, 318, 323 and 328 K, respectively (Fig. 7). From the results it could be seen that A_T , which also signifies the equilibrium binding constant corresponding to the maximum binding energy of the adsorbent, is decreasing as the temperature increased from 298K to 328K. The constant b_T relating to the heat of adsorption of activated tamarind kernel powder for Acid Red 1 at 298, 308, 318, 323 and 328 K is 552.4, 600.4, 668.8, 808.1, and 820.6 J/mg, respectively.

Dubinin-Radushkevich (D-R) isotherm

This considers that adsorbent size is comparable to the micropore size and the adsorption equilibrium relation for a given adsorbate-adsorbent combination can be expressed

independent of temperature by using the adsorption potential (ϵ)

$$\epsilon = RT \ln \left(1 + \frac{1}{C_e} \right) \quad (9)$$

The D-R isotherm assumes a Gaussian-type distribution for the characteristic curve and the model can be described as follows

$$\ln q_e = \ln q_s - B\epsilon^2 \quad (10)$$

Where: q_s is the D-R constant (mol/g) and B gives the activation energy E_A (kJ/mol) per molecule of adsorbate at the moment of its transfer to the solid surface from the bulk solution and can be computed using the equation:

$$E_A = \frac{1}{(2B)^2} \quad (11)$$

Values of q_s and B can be determined through linearization of the D-R isotherm by plotting $\ln q_e$ versus ϵ^2 .

The activation energy E_A reveals the nature of adsorption. Thus, if the value of activation energy E_A is less than 8 KJ/mol, adsorption process is physical; but if it is ranged from 8 to 16 KJ/mol, it is a chemical adsorption.

The Dubinin-Radushkevich parameters B_D and q_D (theoretical isotherm saturation capacity) were calculated from the slopes and intercepts of the linear plots of $\ln q_e$ versus ϵ^2 . The Dubinin Radushkevich adsorption isotherm models for Acid Red 1 at a temperature range of 298K to 328K respectively. From the figures it could be seen that the plots are linear and the correlation coefficient (R^2) values were found to be 0.941, 0.932, 0.974, 0.965, and 0.933 at 298, 308, 318, 323 and 328 K, respectively which indicate that the graphs follow the Dubinin Radushkevich isotherm model. The saturation capacity constant (q_D) of the activated tamarind kernel powder for Acid Red 1 were 13.0, 13.2, 13.1, 13.0 and 12.76 mg/g at 298, 308, 318, 323 and 328 K, respectively (Fig. 8). From the results it could be seen that q_D , is decreasing as the temperature increased from 298 to 328 K. The constant B_D relating to the mean free energy of adsorption of Acid Red 1 on activated tamarind kernel powder at 298, 308, 318, 323 and 328 K is -1×10^{-5} (mol²/J²), -7×10^{-6} , -4×10^{-6} , -2×10^{-6} , and -9×10^{-7} (mol²/J²), respectively.

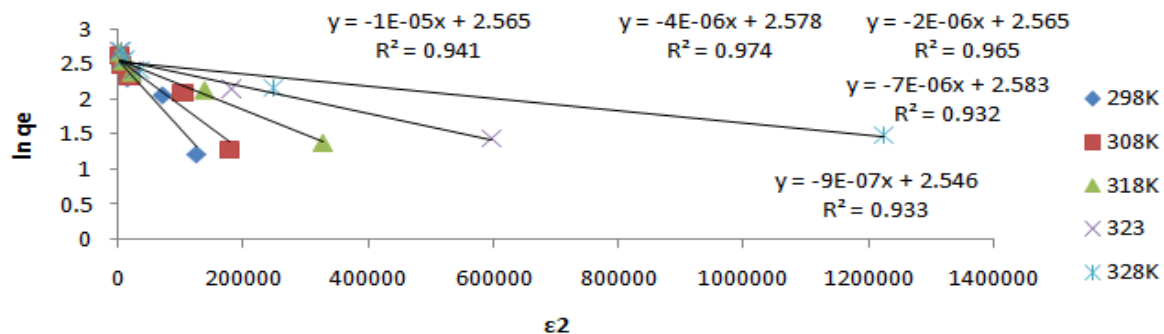


Fig. 8: Dubinin-Radushkevich isotherm model for AR1 adsorption on ATKP

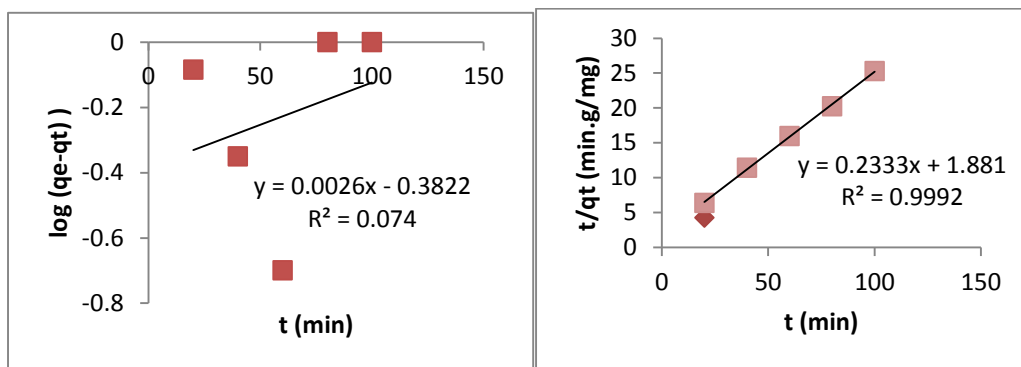


Fig. 9: Pseudo first and second order kinetic model for AR1 adsorption on ATKP

Table 3: Equilibrium data for plotting pseudo first and second order kinetics for AR1 dye adsorption on ATKP

Dye	Time (min)	qt (mg/g)	qe (mg/g)	qe- qt (mg/g)	log (qe- qt) (mg/g)	t/qt (min.g/mg)
AR1	20	3.1	4.0	0.8	-0.1	6.4
	40	3.5		0.5	-0.4	11.4
	60	3.8		0.2	-0.7	16.0
	80	4.0		0	0	20.3
	100	4.0		0	0	25.3

Adsorption kinetics

Fitting an experimental data into different kinetic models enables us to study the adsorption rate, model the process and predict information about adsorbent/adsorbate interaction.

In this study, two different models were used such as the pseudo-first-order (Hashem and El-Khirraigy, 2013; Hameed *et al.*, 2008) and the pseudo-second-order (Ho and Mackay, 2003). Pseudo-first order and pseudo-second order kinetic models described above were used to test the equilibrium data in order to investigate the mechanism of adsorption and potential rate controlling step of the adsorption process. However, in selecting optimum conditions for carrying out full scale batch dye removal processes, information on the kinetics of dye adsorption is required. A kinetic study at different time intervals, constant initial dye concentration and adsorbent dosage was performed and the results obtained.

The pseudo-first and pseudo second order kinetics modelling of Acid Red 1 adsorption onto ATKP are presented. The experimental adsorption capacity of Acid Red 1 is 3.95 mg/L (Fig. 9). The adsorption capacity by using pseudo-first order model was calculated and presented as 2.56 mg/L while that of pseudo-second order model is 2.41 mg/L. The calculated adsorption capacity of the dye by pseudo-second order model was seen to be very close to its respective experimentally determined adsorption capacity. But when the adsorption capacities obtained from the pseudo-first order kinetics were compared with the experimentally determined value, a large difference was observed. The values obtained for the correlation coefficients, R^2 , of the pseudo-first order adsorption model was 0.074. For pseudo-second order kinetics we have R^2 value as 0.999 (Fig. 9). From the above result it could be seen that the R^2 value obtained from the Pseudo-second order kinetic plot is higher than that obtained from the Pseudo-first order adsorption kinetic plot. Thus, the correlation coefficient value and calculated adsorption capacities of all the dyes did not follow the pseudo-first order kinetic model, which suggest that the adsorption of Acid Red 1 on activated tamarind kernel powder is dependent on initial concentration. Hence, pseudo-second order adsorption model is more suitable to describe the adsorption kinetics of Acid Red 1 onto ATKP and this relies on the assumption that adsorption may be the rate-limiting step. The obtained kinetic information has a significant practical value for technological

applications, since kinetic modelling successfully replaces time and material consuming experiments necessary for process equipment design (Gupta and Rastogi, 2017).

Adsorption thermodynamics

Thermodynamic considerations of an adsorption process are necessary to conclude whether the process is spontaneous or not. The Gibb's free energy change, ΔG , indicates the feasibility and spontaneity of a chemical reaction and therefore is an important criterion for spontaneity determination. Both enthalpy (ΔH) and entropy (ΔS) factors must be considered in order to determine the Gibb's free energy of the process. Reactions occur spontaneously at a given temperature if ΔG is a negative quantity (Papita *et al.*, 2010). ΔH determines if the process is exothermic or endothermic; and ΔS determines the increase or decrease in randomness of the process at the solid/solution interface. Reactions occur spontaneously at a given temperature if ΔG is a negative quantity (Okoli *et al.*, 2015). The temperatures used in the thermodynamic study were 298, 308, 318, 323 and 328 K. The values ΔH and ΔS were obtained from the slopes and intercepts, respectively of the Van't Hoff plots (Fig. 10).

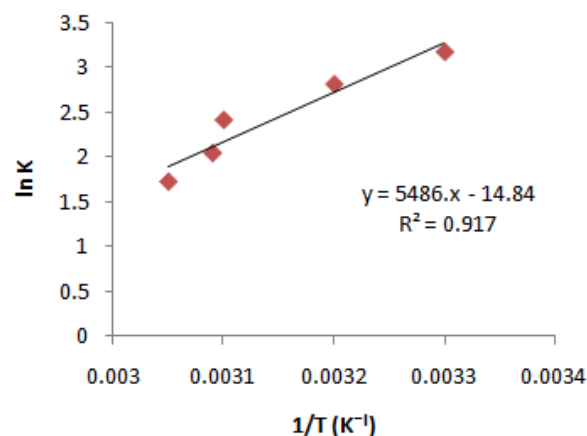


Fig. 10: Van't Hoff plot for thermodynamic studies for AR1 adsorption on ATKP

The negative ΔG values indicate that the process is thermodynamically feasible and spontaneous. The negative ΔH values indicate that the nature of the adsorption process is exothermic indicating that heat is released during the adsorption process. This is also supported by the decrease in the value of adsorption capacity of the adsorbent with the increase in temperature. The negative values of ΔS pointed to a decreased disorder of the solid/solution interface during the adsorption process. However, similar results were obtained in (Okoli *et al.*, 2015).

Conclusion

In this research, adsorption of C.I Acid Red 1 using activated carbonized tamarind kernel powder was successfully carried out. The characterization analysis carried out on the activated carbon indicated that all parameters namely: bulk density, pH, ash content and dry matter were within acceptable range. The Fourier transform infrared spectroscopic analysis carried out on the raw activated tamarind kernel powder indicated the presence of functional groups which include: Hydroxyl, alkanes, alkenes, alkynes, carboxyl, phenols, phosphates, carbonyl, primary and secondary amines, etc.; which constitute very important adsorption sites on the adsorbent surface. The FTIR analysis carried out on the dye-adsorbed activated tamarind kernel powder indicated the presence of some functional groups which did not appear in the FTIR spectrum of raw ATKP. They include: open chain azo groups, quinones, conjugated ketones, sulphonates, aromatic ethers, aromatic nitro groups etc. The effect of the different parameters namely: pH, adsorbent dosage, initial dye concentration, contact time and temperature indicated that the adsorption of Acid Red 1 from wastewater using activated tamarind kernel powder is independent on this factors. From the four equilibrium isotherms tested in this research the order in which the data obtained best fits the isotherm models are Temkin >Langmuir > Dubinin Radushkevich > Freundlich. From the Adsorption kinetic models, Pseudo-Second order kinetic model offered the best description of the adsorption kinetics modelling carried out. From the thermodynamic studies, it could be inferred that the adsorption of Acid Red 1 on activated tamarind kernel powder is a physical process (physisorption) due to the fact that the activation energy (E_A) value was less than 8kJ/mol and hence the adsorbent can be easily regenerated and re-used. It is also feasible and spontaneous due to negative value of the Gibb's free energy (ΔG). The negative change in enthalpy (ΔH) value revealed the exothermic nature of the adsorption process. The negative change in entropy (ΔS) values of the system suggests the decrease in adsorbate concentration in solid-solution interface indicating thereby the increase in adsorbate concentration onto the solid phase. This is the normal consequence of the physical adsorption phenomenon, which takes place through electrostatic interactions as reported in (Seswati and Uday, 2012).

Conflict of Interest

Authors declare that there is no conflict of interest.

References

Abechi SE 2006. Adsorption Characteristics of Ti (IV) and Zn(II) Oxide Coated Activated Carbon from Walnut Shells. An M.Sc. Thesis, Department of Chemistry, Ahmadu Bello University, Zaria.

Akbal F 2005. Heterogeneous Do-Do models of water adsorption on carbons. *J. Colloid and Interface Sci.*, 286: 455-458.

Andre LC, Alexandro MM, Eurica MN, Marcos HK, Marcos RG, Alessandro CN, Tais LS, Juliana CG & Victor CA 2011. Activated carbon of high surface area produced

from coconut shell: Kinetics and equilibrium studies from the methylene blue adsorption. *Chemical Engineering Journal*, 174: 117-125.

American Society for Testing & Materials 1996. Standard Method for the Determination of pH value in Biomass, Philadelphia, PA: 11(05).

American Society for Testing & Materials 2003. Standard Method for the Determination of Ash in Biomass, Philadelphia PA: 11(05).

Bhatti I, Qureshi K, Kazi R & Ansari AK 2007. Physical and chemical analysis of activated carbon prepared from sugarcane daggasse and use for sugar decolonization. *World Acad. Sci., Engr. and Techn.*, 34: 194-198.

Bhattacharyya & Sharma 2005. Photocatalytic degradation of two selected dye derivatives, chromotrope 2B and Amido Black 10B, in aqueous suspensions of titanium dioxide. *Journal of Dyes and Pigments*, 65(1): 1-88.

Bulut Y & Aydin H 2006. A kinetics and thermodynamics study of methylene blue adsorption on wheat shells. *Elsevier Journal of Desalination*, 194: 259-267.

Cheremisinoff NP & Chermisinoff PN 1993. Carbon Adsorption for Pollution Control; Prentice Hall, Englewood Cliffs, NJ.

Dada AO, Olalekan AP, Olatunya AM & Dada O 2012. Langmuir, freundlich, temkin and dubinin-radushkevich isotherms studies of equilibrium sorption of Zn^{2+} unto phosphoric acid modified rice husk. *IOSR J. Appl. Chem.*, 3(1): 38-45.

Deshuai S, Zhongyi Zhang, Mengling W & Yude W 2013. Adsorption of reactive dyes on activated carbon developed from *Enteromorpha prolifera*. *Am. J. Anal. Chem.*, 4: 17-26.

Erhan D, Kobya M, Elif S & Tuncay O 2004. Adsorption kinetics for the removal of chromium (VI) from aqueous solutions on the activated carbons prepared from agricultural wastes. *Journal of Water Research*, 30(4): 533-540.

El-Hendawy AA, Alexander RJ & Andrews GF 2008. Effect of activation schemes on porous surface and thermal properties of activated carbons prepared from cotton stalk. *J. Anal. Appl. Pyrolysis*, 82: 272-278.

Gimba CE, Ocholi OJ, Egwaikhida PA, Muiyiwa T & Akporhonor EE 2009. New raw material for activated carbon. I. Methylene blue adsorption on activated carbon prepared from *Khaya senegalensis* fruits. *Nig. J. Scientific Res.*, 36(1): 107-114.

Gupta VK & Rastogi A 2007. Biosorption of lead from aqueous solutions by green alga spirogyra species. kinetics and equilibrium studies. *J. Colloid and Interface Sci.*, 296: 59-63.

Ho YS & McKay G 2003. Pseudo-second order model for sorption processes. *Process Biochemistry Journal*, 34(5): 451-465.

Joseph TN & Philomena KI 2011. Copper (II) uptake by adsorption using palmyra palm nut. *J. Advance Appl. Sci. Res.*, 2(6): 166-175.

Kesari KK, Verma HN & Behari J 2011. Physical Methods in Wastewater Treatment: Sono Chemistry: Environmental Science and Engineering Application in Wastewater, LAP LAMBERT Academic Publishing, 152.

Krishnaiah A, Kayani F, Sankara RVS, Boddu VM & Subbaiah MV 2008. Biosorption of Cr(VI) from aqueous solutions using *Trametes versicolor* polyporus fungi. *Electronic Journal of Chemistry*, 5(3): 499-510.

Langmuir I 1916. The constitution and fundamental properties of solids and liquids. *J. Am. Chem. Soc.*, 38: 2221-2295.

Ladhe UV, Wankhede SK, Patil VT & Patil PR 2011. Adsorption of erichrome black t from aqueous solutions

- on activated carbon prepared from mosambi peel. *J. Appl. Sci. Environ. Sanitation*, 6: 149-154.
- Mahamadi C & Torto N 2007. A comparative study of the kinetics of nickel biosorption by river system. *Electr. J. Environ. Sci. and Techn.*, 5(2): 275-285.
- Malik PK 2003. Use of activated carbons prepared from sawdust and rice husk for adsorption of acid dyes: A case study of acid yellow 36. *Elsevier Journal of Dyes and Pigments*, 56: 239-249.
- Mattson JS & Mark HB 1971 *Water Quality Measurement: The Modern Analytical Techniques* (Pollution Engineering and Technology). Marcel Dekker Publishers, New York.
- Oladunni N, Agbaji EB & Idris SO 2012. Removal of Pb²⁺ and Ni²⁺ from aqueous solutions by adsorption onto activated locust bean (*Parkia biglobosa*) husk. *Archives of Appl. Sci. Res.*, 4(5): 2161-2173.
- Okoli CA, Onukwuli CD, Okey-Onyesolu CE & Okoye CC 2015. Adsorptive removal of dyes from synthetic waste water using activated carbon from tamarind seed. *European Scientific Journal*, 11(18): 190-221.
- OMRI 2002. Activated Carbon Processing. National Organic Standards Board of Technical Advisory Panel Review for the USDA. National Organic Program, pp. 1-14.
- Ozacar M & Sengil IA 2003. Adsorption of reactive dyes on calcined alunite from aqueous solutions. *Journal Hazardous Materials*, 98: 211-224.
- Palanisamy PN, Agalya A & Sivakumar P 2013. Equilibrium uptake and sorption dynamics for the removal of reactive dyes from aqueous solution using activated carbon prepared from *Euphorbia tirucalli* L wood. *Indian J. Chem. Techn.*, 20: 245-251.
- Pons MP & Fuste CM 1993. Uranium uptake by immobilized cells of pseudomonas strain. *J. Appl. Microbio. and Biotechn.*, 39(4-5): 661-665.
- Saswati G & Uday CG 2005. Studies on adsorption behaviour of Cr(VI) onto synthetic hydrous stannic oxide. *Water Resources*, 13(4): 597-602, (www.wrc.org.za)
- Shanathi & Mahalakshmi T 2012. Studies on the removal of malachite green and methylene blue dyes from aqueous solutions of their binary mixture by adsorption over commercial activated carbon and tamarind kernel powder. *Int. J. Res. Pharmacy and Chem.*, 2(2): 289-298.
- Sun Q & Yang L 2003. The adsorption of basic dyes from aqueous solution on modified peat-resin particle. *Elsevier J. Water Res.*, 37(7): 1535.
- Suresh DS, Thomas KA, Mohan PN & Damodaran AD 1994. Alteration of ilmenite in the Manavalakurichi Deposit, India. *Clays and Clay Minerals Journal*, 42(5): 567 - 571.
- Saradhi BV, Rao SRK, Kumar YP, Vijetha P, Rao KV & Kalyami G 2010. Applicability of Langmuir and Freundlich theory for biosorption of chromium from aqueous solution using test of sea urchins. *Int. J. Chem. Engr. Res.*, 2(2): 139-148.
- Vijayakumar G, Tamilarasan R & Dharmendirakumar M 2012. Adsorption, kinetic, equilibrium and thermodynamic studies on the removal of basic dye rhodamine-B from aqueous solution by the use of natural adsorbent. *J. Material and Environ. Sci.*, 3(1): 157-170.
- Papita S, Shamik C, Gupta S, Kumar I & Kumar R 2010. Assessment on the removal of malachite green using tamarind fruit shell as biosorbent. *CLEAN-Soil, Air, Water*; 38(5-6): 437-445.
- Hashem A & El-Khiraigy K 2013. Bioadsorption of Pb(II) onto anethum graveolens from contaminated wastewater: Equilibrium and kinetic studies. *J. Environmental Protection*, 4: 108-119.
- Hameed BH, Tan IAW & Ahmad AL 2008. Adsorption isotherm, kinetic modeling and mechanism of 2,4,6-trichlorophenol on coconut husk-based activated carbon. *Chemical Engineering Journal*, 144: 235-244.
- Ocholi O 2006. Studies on the preparation and adsorption of activated carbon matrices from *Delonix regia* pods and *Khaya senegalensis* fruits. An M.Sc. Thesis, Department of Chemistry, Ahmadu Bello University, Zaria.
- Shakirullah M, Habib-ur-Rehman IA, Sher S & Hameedullah G 2006. Sorption studies of nickel ions onto sawdust of *Dalbergia sisso*. *J. Chinese Chem. Soc.*, 53: 1045-1052.